

Weak localization in $\text{Ga}_{1-x}\text{Mn}_x\text{As}$: Evidence of impurity band transport

L. P. Rokhinson and Y. Lyanda-Geller

Department of Physics and Birk Nanotechnology Center, Purdue University, West Lafayette, Indiana 47907, USA

Z. Ge, S. Shen, X. Liu, M. Dobrowolska, and J. K. Furdyna

Department of Physics, University of Notre Dame, Notre Dame, Indiana 46556, USA

(Received 28 February 2007; revised manuscript received 12 July 2007; published 12 October 2007)

We report the observation of negative magnetoresistance in the ferromagnetic semiconductor $\text{Ga}_{1-x}\text{Mn}_x\text{As}$, $x=0.05-0.08$, at low temperatures ($T < 3$ K) and low magnetic fields ($0 < B < 20$ mT). We attribute this effect to weak localization. Observation of weak localization strongly suggests impurity band transport in these materials, since for valence band transport one expects either weak antilocalization due to strong spin-orbit interactions or total suppression of interference by intrinsic magnetization. In addition to the weak localization, we observe Altshuler-Aronov electron-electron interaction effects in this material.

DOI: [10.1103/PhysRevB.76.161201](https://doi.org/10.1103/PhysRevB.76.161201)

PACS number(s): 75.50.Pp, 71.23.-k, 73.20.Fz

Dilute magnetic semiconductors (DMS) form a bridge between conventional ferromagnetic materials and semiconductors, with the promise of electrostatic tailoring of magnetic properties.¹ If enabled to operate at room temperature, the DMS materials will play a central role in the rapidly developing field of spintronics, with applications ranging from sensors to memories and quantum computing. In Mn-based DMSs such as GaMnAs ,²⁻⁴ the ferromagnetism is carrier-mediated, so that their magnetic properties are tightly related to the nature of electronic transport.

The principal unresolved issue in the physics of GaMnAs concerns the roles of valence and impurity bands. The Zener model of ferromagnetism (which becomes equivalent to the RKKY approach) has been proposed by Dietl,⁵ and developed by others⁶⁻⁸ based on the assumption of hole transport in the valence band in this and related materials. Alternatively, it has been suggested that the holes in GaMnAs reside in the impurity band.⁹⁻¹² Recent optical studies provide strong evidence of impurity band formation.^{13,14} Understanding the origin of electronic states participating in transport—which bear on the physical origin of ferromagnetism in III-Mn-V alloys—clearly constitutes the key to achieving higher T_c in DMSs.

In this paper, we demonstrate that low-temperature conduction in GaMnAs is inconsistent with valence band transport. We observe a peak in magnetoresistance at very small magnetic fields ($B < 20$ mT), which is independent of orientation of B with respect to the ferromagnetic easy axis and to the direction of the electric current. The peak appears below 3.4 K and increases at lower temperatures. We attribute this effect to the anomalous negative magnetoresistance of the Aharonov-Bohm (AB) origin.^{15,16} The shape and magnitude of the peak is consistent with weak localization (WL)^{17,18} in a three-dimensional (3D) conductor with weak spin-orbit interaction. Holes in the valence band, on the contrary, experience strong spin-orbit interaction, which would lead to weak antilocalization (positive magnetoresistance)^{19,20} in the absence of ferromagnetic order or in suppression of interference effects below T_c . In addition to WL we observe a field-independent increase of resistance at $T < 8$ K, a signature of Altshuler-Aronov (AA) electron-electron interaction effect

on resistivity.²¹ Such temperature dependent AA contribution is almost an order of magnitude larger than the magnitude of the magnetoresistance peak, as it should be in conventional 3D disordered conductors.

The GaMnAs wafers were grown by molecular beam epitaxy (MBE) on semi-insulating (001) GaAs substrates. Prior to GaMnAs deposition a 120 nm GaAs buffer was grown at 590 °C, followed by a 2 nm GaAs buffer grown at 275 °C. 100 nm of $\text{Ga}_{1-x}\text{Mn}_x\text{As}$ was deposited next, with $x = 0.02, 0.05, 0.65,$ and 0.08 . We will refer to those as 2%, 5%, 6.5%, and 8% Mn samples. The Curie temperatures for these wafers are in the range $60 \text{ K} < T_c < 100 \text{ K}$. The measurements were performed on large Hall bars (a few mm) oriented along the [110] crystallographic direction. Longitudinal and Hall resistances were measured using the standard four-probe lock-in technique with 10 nA excitation current in a dilution refrigerator (0.05–1.2 K) and in a pumped ⁴He system (1.2–300 K). Magnetic fields in the dilution refrigerator were generated by a home-made two-axis magnet, which in combination with a rotator allows us to point the magnetic field in an arbitrary direction. In the following B_\perp refers to the field oriented normal to the sample surface ($B_\perp \parallel [001]$); and for in-plane orientations the field direction will be indicated explicitly (for example, $B_{[110]} \parallel [110]$).

Temperature dependence of resistivity at zero magnetic field is plotted in Fig. 1 for 5% Mn and 6.5% Mn samples. As the temperature is decreased in the paramagnetic phase, the resistance increases and reaches a maximum around T_c , which can be attributed to the enhanced spin disorder scattering. Deep in ferromagnetic phase ($T \ll T_c$) the 2% Mn sample becomes insulating (resistivity exhibits hopping transport). In contrast, samples with $>4\%$ Mn show metallic behavior at low temperatures. However, the resistivity does not saturate as $T \rightarrow 0$, but reaches a minimum at ~ 8 K and then slowly increases as the temperature decreases down to the lowest $T=30$ mK. We do not expect any resistance change due to ferromagnetic ordering at these temperatures, since thermodynamically magnetization reaches 99% of its $T=0$ value already at $T=0.2T_c \approx 10$ K. Moreover, an increase in ferromagnetic order should reduce the resistivity, as in the $8 \text{ K} < T < T_c$ temperature range.

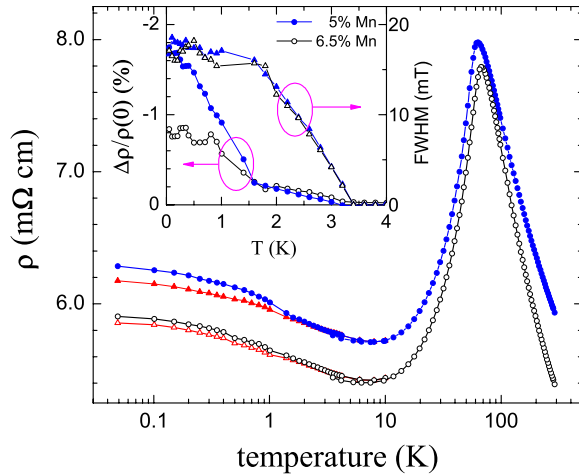


FIG. 1. (Color online) Temperature dependence of resistivity at $B=0$ plotted for samples with 5% Mn (solid dots) and 6.5% Mn (open dots). Triangles are measured at $B_{\perp}=30$ mT. In the inset the height $[\rho(30 \text{ mT})-\rho(0)]/\rho(0)$ (dots) and the full width at half maximum (FWHM) (triangles) of magnetoresistance peak seen in Fig. 2 are plotted as a function of temperature.

Weak enhancement of resistivity at low temperatures in disordered conductors is usually associated with quantum interference and/or interaction effects. Such interference effects are sensitive to external magnetic fields, and we indeed observe that the application of a small field of $B_{\perp}=30$ mT reduces resistivity at $T<3.4$ K. The difference in resistivity $\rho(30 \text{ mT})-\rho(0)$ is plotted in the inset of Fig. 1. This zero-field enhancement of resistivity reveals itself as a narrow peak in magnetoresistance. In Fig. 2 magnetoresistance at different T is plotted for an out-of-plane magnetic field B_{\perp} . At $T>3.4$ K there is no change in resistivity in the $-100 \text{ mT}<B_{\perp}<100 \text{ mT}$ range. At $T\approx 3.4$ K a peak appears at $B_{\perp}=0$. The height of the peak then gradually increases as the temperature decreases, and approaches 1–2% of the over-

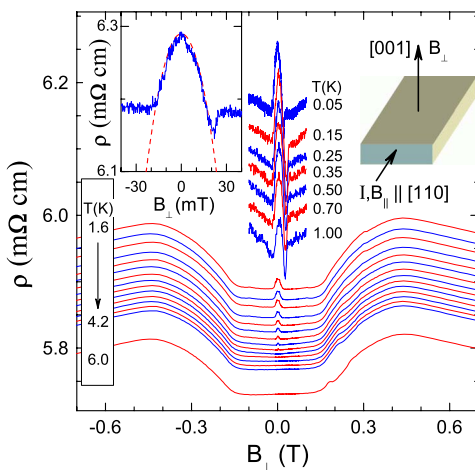


FIG. 2. (Color online) Magnetoresistance in 5% Mn sample plotted at different temperatures $0.05 < T < 6$ K. Between 1.6 K and 4.2 K $\rho(B)$ is plotted at 0.2 K intervals. In the inset zero-field peak at 50 mK is enlarged. The dashed curve is a fit with $\rho(B)-\rho(0) \propto B^2$.

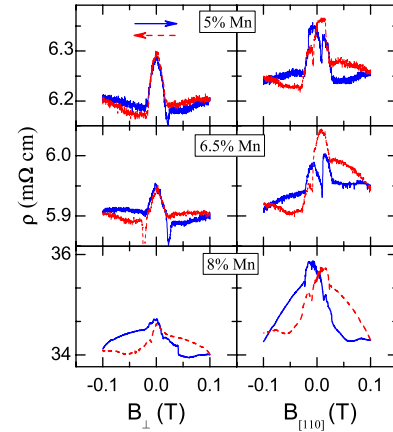


FIG. 3. (Color online) Magnetoresistance plotted for three samples with different Mn concentrations for normal (B_{\perp}) and in-plane ($B_{[110]}$) magnetic fields. Solid (dashed) curves are for magnetic field sweeps up (down). Data for $B_{\perp}(B_{[110]})$ were measured at 66 mK (23 mK).

all resistivity at $T=30$ mK. The peak width also increases with decreasing T , and almost saturates for $T<1$ K.

The height and shape of the zero-field peak is independent of the orientation of magnetic field. In Fig. 3 we plot magnetoresistance as a function of the out-of-plane B_{\perp} and in-plane $B_{[110]}$ fields for three samples with different Mn concentrations. The overall shape of magnetoresistance is very different for the two field orientations, and exhibits a hysteretic behavior. The zero-field peak, however, has no hysteresis and has a similar height and width for both field orientations, which suggests that its origin is not related to ferromagnetic ordering. This feature is emphasized in Fig. 4, where both R_{xx} and the planar Hall effect (PHE) are plotted for different orientations of the in-plane magnetic field. The jumps in PHE indicate switching of magnetic domains, which produce corresponding spikes in magnetoresistance, but do not change the overall shape of the zero-field peak. We also observe a zero-field enhancement of the PHE, similar to the peak in magnetoresistance. This behavior is consistent with the PHE resulting from inhomogeneities of current flow and reflects the corresponding enhancement of R_{xx} .

We now discuss the experimental data. The only known physics that can explain a low magnetic field magnetoresistance that is independent of the magnetic field orientation relative to the current and to crystallographic axes is the phenomenon of weak localization (WL), which leads to anomalous magnetoresistance arising from the Aharonov-Bohm effect. There are several distinct experimental features which indicate that the observed effect is indeed related to WL. (i) The zero-field peak gradually disappears with increasing temperature as the phase breaking processes intensify, thus destroying WL. (ii) Similar temperature dependence characterizes also the magnetic-field-independent background. This behavior is characteristic to the Altshuler-Aronov (AA) electron-electron interactions effect on resistivity that accompanies WL in disordered conductors at low temperatures. Indeed, the AA effect is not destroyed (to a leading order) by the Aharonov-Bohm magnetic flux passing through electron trajectories, and its magnetic field depen-

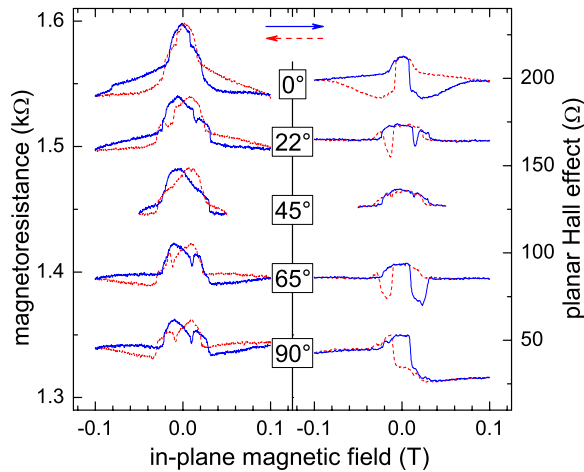


FIG. 4. (Color online) Magnetoconductance (left panel) and planar Hall effect (right panel) shown for different orientations of in-plane magnetic field in the 6.5% Mn sample. All curves except $\alpha=90^\circ$ are offset for clarity. Angle $\alpha=0^\circ$ corresponds to $B\parallel[110]$, $\alpha=45^\circ$ to $B\parallel[100]$ (the easy axis of magnetization), and $\alpha=90^\circ$ to $B\parallel[1\bar{1}0]$. Current $I\parallel[110]$. Solid (dashed) curves are for magnetic field sweeps up (down).

dence due to spin arises only in rather strong magnetic fields.²² Furthermore, in 3D conductors the AA contribution to magnetoconductance should exceed the WL contribution by an order of magnitude. The experimentally measured ratios are 4 and 11 for the wafers with 5% and 6% Mn, respectively. (iii) The value of magnetoconductance is also consistent with the WL physics. Furthermore, from the suppression of the WL peak at 20 mT we estimate the phase breaking length to be $l_\phi \approx 0.1$ microns. This estimate is consistent with the inelastic phase breaking length extracted from universal conduction fluctuations in similar materials.^{23,24} (iv) The shape of the zero-field peak is consistent with theoretically expected B^2 dependence (see inset in Fig. 2).

We thus attribute the zero-field peak in magnetoconductance to the WL effect. This observation is intriguing, because GaMnAs is a magnetic alloy, so that magnetic interactions must coexist with WL, which limits their strength. Furthermore, the negative sign of the observed magnetoconductance brings certain restrictions on the properties of charge carriers contributing to the resistivity.

From general symmetry principles the WL correction to conductivity for charge carriers with spin (angular momentum) 3/2 is

$$\Delta\sigma \propto -\frac{1}{4} \left(-S_0 + \sum_{i=1}^1 T_{1,i} - \sum_{i=2}^2 Q_{2,i} + \sum_{i=3}^3 S_{3,i} \right), \quad (1)$$

where S_0 is the singlet contribution to conductivity of interfering electron waves with total spin zero and $T_{1,i}$, $Q_{2,i}$, and $S_{3,i}$ are triplet, quintuplet, and septuplet contributions. They arise from the total angular momenta 1, 2, and 3, respectively, i being the projection of angular momentum on the quantization axis.

When orbital (Aharonov-Bohm) effects suppress the interference contributions, one observes either a negative or a

positive magnetoconductance, depending on the relative importance of the multiplets and singlet. This relative importance is determined by the strength of spin-dependent interactions. A negative magnetoconductance requires that spin and spin-orbit scattering are negligible, that almost no intrinsic spin-orbit interactions present, and that charge carriers are not affected by a strong Zeeman effect and/or ferromagnetism. If these conditions are satisfied, the Aharonov-Bohm flux suppresses localization of electrons, leading to negative magnetoconductance, which is defined by the sum of singlet, triplet, quintuplet, and septuplet contributions. We note that when all spin-dependent interactions are absent, each of the multiplets contributing to WL is equal to the singlet, leading to a localizing correction, $\Delta\sigma \propto -S_0$, and to negative magnetoconductance. However, if strong spin-orbit effects completely suppress all multiplet contributions, the remaining singlet contribution will lead to antilocalization, $\Delta\sigma \propto \frac{1}{4}S_0$, and, correspondingly, to a positive magnetoconductance.

GaMnAs is characterized by several magnetic interactions: Spins are affected by average magnetization in the ferromagnetic phase, by scattering off magnetic fluctuations due to Mn, by domain walls and other magnetization inhomogeneities, and finally by intrinsic spin-orbit interactions and spin-orbit scattering. Observation of WL allows us to make conclusions about dominant hole scattering mechanisms. In particular, we conclude that scattering by magnetic fluctuations cannot be dominant. Otherwise the singlet and multiplet terms, both affected by such scattering, would be entirely suppressed, leading to the absence of interference effects. Thus it is the very strong positional disorder rather than magnetic scattering that dominates the scattering mechanism, limiting the mean free path.

In contrast to scattering off magnetic fluctuations, average ferromagnetic magnetization of GaMnAs must have a profound effect on the interference terms, entirely suppressing contributions with antiparallel spins in singlet and multiplet states. If S_0 is entirely suppressed, the only contributions to weak localization arise from multiplets, resulting in negative magnetoconductance. The remaining magnetic interactions: Domain walls and other smooth magnetic inhomogeneities, and various types of spin-orbit interactions, can only affect multiplet terms with nonzero projections of angular momentum.²⁵ If these magnetic interactions are weak, then a negative magnetoconductance can indeed be observed, as seen experimentally.

We can now set a restriction on the origin of carriers that contribute to the conductivity. If the contributions were coming from valence band holes in GaMnAs, then strong spin-orbit interactions of total angular momentum of holes with their kinetic momentum k would result in spin dephasing (scattering) times of the order of the transport scattering time. This would lead to the total suppression of multiplet terms, resulting in a positive magnetoconductance similar to that observed in nonmagnetic p -type materials.²⁶ In contrast, for localized states no spin orbit interaction relevant for WL exists. Metallic impurity band is an intermediate case between wide valence band and localized states, and spin-orbit interactions are expected to be weaker than in valence band. Thus the spin-orbit effects in the impurity band have only limited impact on multiplet terms, in agreement with the observed negative magnetoconductance.

Finally, we would like to point out several unusual features observed in our experiments. Typically a negative magnetoresistance in 3D disordered nonmagnetic conductors has B^2 field dependence at low B , which smoothly evolves into \sqrt{B} at higher B (at $l_m \sim l_\phi$, where l_m is the magnetic length). In our samples, however, instead of such gradual change of magnetoresistance with field we observe an abrupt suppression of the effect. A related feature is the T dependence of the width of the magnetoresistance peak. From $l_m \sim l_\phi$ crossover one expects that the peak will broaden with increasing temperature (since $l_m \propto B^{-1/2}$ and $l_\phi \propto T^{-1}$). In our data, however, we observe just the opposite: The magnetoresistance peak narrows as the temperature increases. We analyzed several mechanisms which can potentially lead to the suppression of WL and are enhanced at higher temperatures. In weak magnetic fields the average spin inside the domains begin to tilt away from the easy axis, and the resulting spin texture will then act as an effective Berry's phase. This suppression mechanism²⁵ should not be present for the field aligned along the [100] (i.e., the easy axis) direction. Experimentally,

however, the peak for $B \parallel [100]$ is the same as for the other field directions; see Fig. 4. Also, the observation of domain switching within the WL peak rules out the possibility that the suppression of WL is caused by domain walls.

In conclusion, we have observed unexpected negative magnetoresistance at small magnetic fields in GaMnAs, which we attribute to weak localization. We also observe weak temperature dependence of resistivity which we ascribe to the Altshuler-Aronov electron-electron interactions effect. The sign of magnetoresistance indicates that transport in GaMnAs cannot originate from valence band holes, but must be attributed to holes in the impurity band. Observation of interference effects in resistivity at high (>4%) Mn concentrations indicates that the hole transport is diffusive.

Recently, observation of weak localization in GaMnAs has also been reported by Neumaier *et al.*²⁷

The work was supported by the NSF under Grant No. ECS-0348289 (L.P.R.) and Grant No. DMR-0603752 (Notre Dame).

-
- ¹J. Furdyna, J. Appl. Phys. **64**, R29 (1988).
²H. Ohno, A. Shen, F. Matsukura, A. Oiwa, A. Endo, S. Katsumoto, and Y. Iye, Appl. Phys. Lett. **69**, 363 (1996).
³H. Ohno, Science **281**, 951 (1998).
⁴D. V. Baxter, D. Ruzmetov, J. Scherschligt, Y. Sasaki, X. Liu, J. K. Furdyna, and C. H. Mielke, Phys. Rev. B **65**, 212407 (2002).
⁵T. Dietl, A. Haury, and Y. M. d'Aubigné, Phys. Rev. B **55**, R3347 (1997).
⁶T. Jungwirth, W. A. Atkinson, B. H. Lee, and A. H. MacDonald, Phys. Rev. B **59**, 9818 (1999).
⁷M. Jain, L. Kronik, J. R. Chelikowsky, and V. V. Godlevsky, Phys. Rev. B **64**, 245205 (2001).
⁸D. J. Priour, E. H. Hwang, and S. Das Sarma, Phys. Rev. Lett. **92**, 117201 (2004).
⁹M. Berciu and R. N. Bhatt, Phys. Rev. Lett. **87**, 107203 (2001).
¹⁰A. Chattopadhyay, S. Das Sarma, and A. J. Millis, Phys. Rev. Lett. **87**, 227202 (2001).
¹¹G. Alvarez and E. Dagotto, Phys. Rev. B **68**, 045202 (2003).
¹²P. Mahadevan and A. Zunger, Phys. Rev. B **69**, 115211 (2004).
¹³V. F. Sapega, M. Moreno, M. Ramsteiner, L. Daweritz, and K. H. Ploog, Phys. Rev. Lett. **94**, 137401 (2005).
¹⁴K. S. Burch, D. B. Shrekenhamer, E. J. Singley, J. Stephens, B. L. Sheu, R. K. Kawakami, P. Schiffer, N. Samarth, D. D. Awschalom, and D. N. Basov, Phys. Rev. Lett. **97**, 087208 (2006).
¹⁵B. L. Altshuler, D. Khmel'nitskii, A. I. Larkin, and P. A. Lee, Phys. Rev. B **22**, 5142 (1980).
¹⁶A. Kawabata, Solid State Commun. **34**, 431 (1980).
¹⁷E. Abrahams, P. W. Anderson, D. C. Licciardello, and T. V. Ramakrishnan, Phys. Rev. Lett. **42**, 673 (1979).
¹⁸L. Gor'kov, A. Larkin, and D. Khmel'nitskii, Pis'ma Zh. Eksp. Teor. Fiz. **30**, 248 (1979).
¹⁹B. L. Altshuler, A. G. Aronov, A. I. Larkin, and D. E. Khmel'nitskii, Zh. Eksp. Teor. Fiz. **81**, 768 (1981) [Sov. Phys. JETP **54**, 411 (1981)].
²⁰Y. Lyanda-Geller, Phys. Rev. Lett. **80**, 4273 (1998).
²¹B. L. Altshuler and A. G. Aronov, JETP Lett. **30**, 482 (1979).
²²P. A. Lee and T. V. Ramakrishnan, Phys. Rev. B **26**, 4009 (1982).
²³K. Wagner, D. Neumaier, M. Reinwald, W. Wegscheider, and D. Weiss, Phys. Rev. Lett. **97**, 056803 (2006).
²⁴L. Vila, R. Giraud, L. Thevenard, A. Lemaître, F. Pierre, J. Dufour, D. Mailly, B. Barbara, and G. Faini, Phys. Rev. Lett. **98**, 027204 (2007).
²⁵Y. Lyanda-Geller, I. L. Aleiner, and P. M. Goldbart, Phys. Rev. Lett. **81**, 3215 (1998).
²⁶S. J. Papadakis, E. P. DePoortere, H. C. Manoharan, J. B. Yau, M. Shayegan, and S. A. Lyon, Phys. Rev. B **65**, 245312 (2002).
²⁷D. Neumaier, K. Wagner, S. Geissler, U. Wurstbauer, J. Sadowski, W. Wegscheider, and D. Weiss, arXiv:cond-mat/0703053v1 (unpublished).